Electronic Supplementary Information

Controlled Oxygen Vacancies Engineering on In_2O_{3-x}/CeO_{2-y} nanotube for Highly Selective and Efficient Electrocatalytic Nitrogen Reduction Reaction

Zengyao Wang[1], Wenzhi Fu[1], Jiangwen Liao[2], Juncai Dong[2], Peiyuan Zhuang[1], Ziyi Cao[1], Zhuolin Ye[1], Jiangyue Shi[1], Mingxin Ye[1]*

[1] Institute of Special Materials and Technology, Fudan University, Shanghai 200433, China

[2] Beijing Synchrotron Radiation Facility, Institute of High Energy Physics, Chinese Academy of Science, Beijing 100049, China

E-mail: mxye@fudan.edu.cn

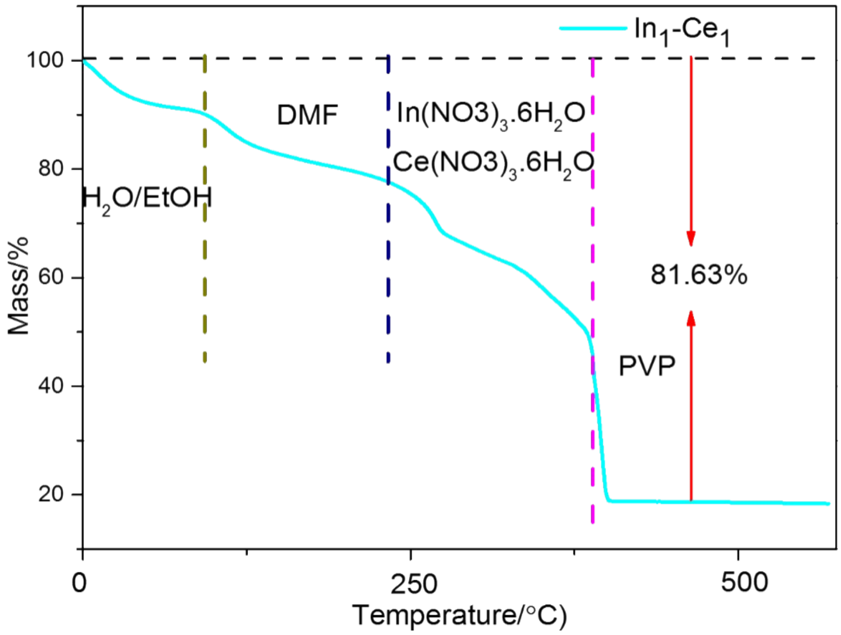

Figure S1. TGA curve of the catalyst In_1-Ce_1 under the air atmosphere (the total flow rate was 20 mL/min).

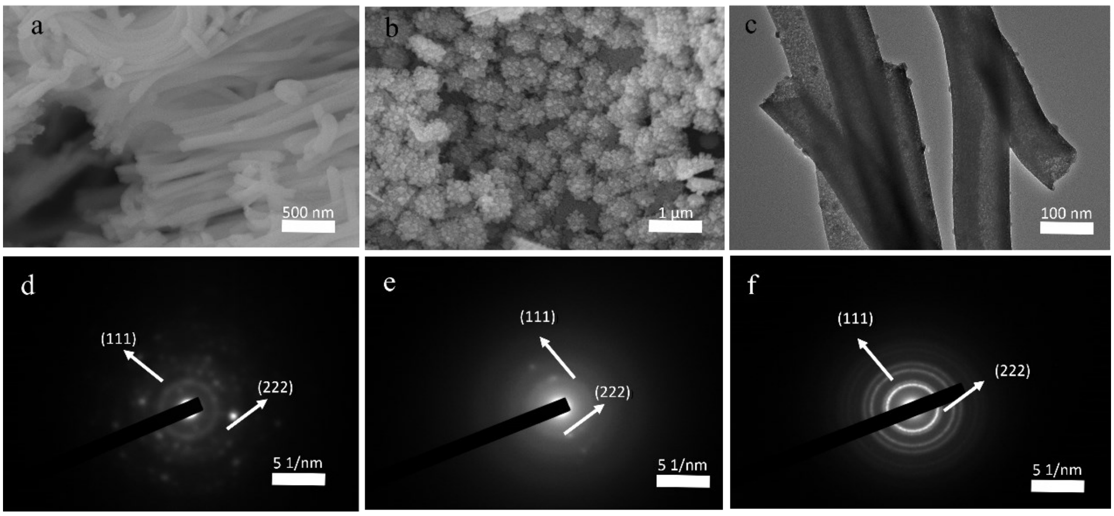

Figure S2. SEM images of the catalyst CeO_2 (a) and catalyst In_2O_3 (b). (c) TEM image of the catalyst In_1-Ce_1. SAED images of In_2-Ce_1 (d), In_1-Ce_1 (e) and In_1-Ce_2 (f).

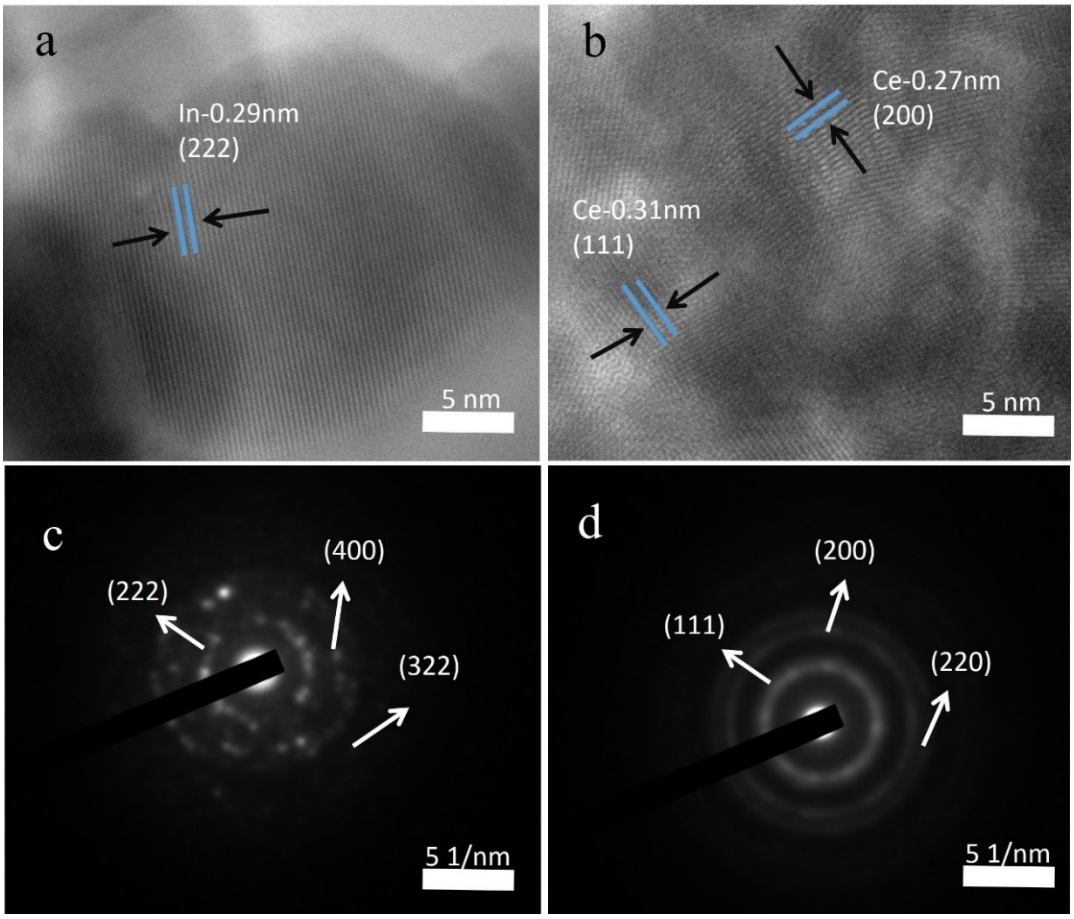

Figure S3. HRTEM images of the catalyst In_2O_3 (a) and the catalyst CeO_2 (b). SAXD images of the catalyst In_2O_3 (c) and catalyst CeO_2 (d).

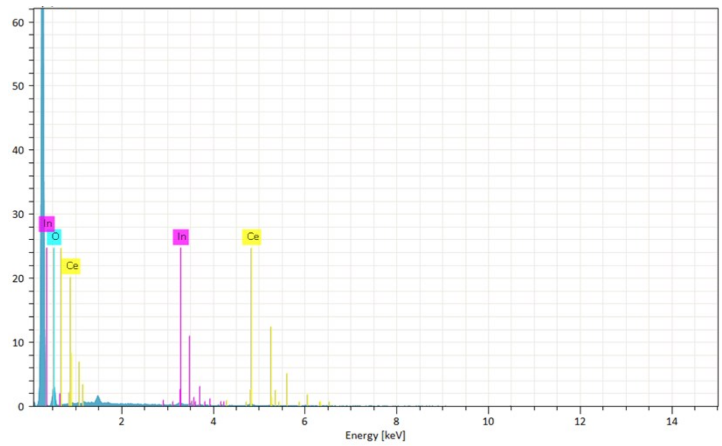

Element	At. No.	Line s.	Netto	Mass [%]	Mass Norm. [%]	Atom [%]	abs. error [%] (1 sigma)	abs. error [%] (2 sigma)	abs. error [%] (3 sigma)	rel. error [%] (1 sigma)	rel. error [%] (2 sigma)	rel. error [%] (3 sigma)
Oxygen	8	K-Serie	2131	12.24	47.65	87.86	2.31	4.62	6.93	18.87	37.74	56.61
Indium	49	L-Serie	1374	6.19	24.12	6.20	0.30	0.59	0.89	4.78	9.57	14.35
Cerium	58	L-Serie	852	7.25	28.24	5.95	0.38	0.75	1.13	5.17	10.34	15.51
Nitrogen	7	K-Serie	0	0.00	0.00	0.00	0.00	0.00	0.00	10.00	20.00	30.00
			Sum	25.68	100.00	100.00						

Figure S4. EDX spectrum of the In_1-Ce_1.

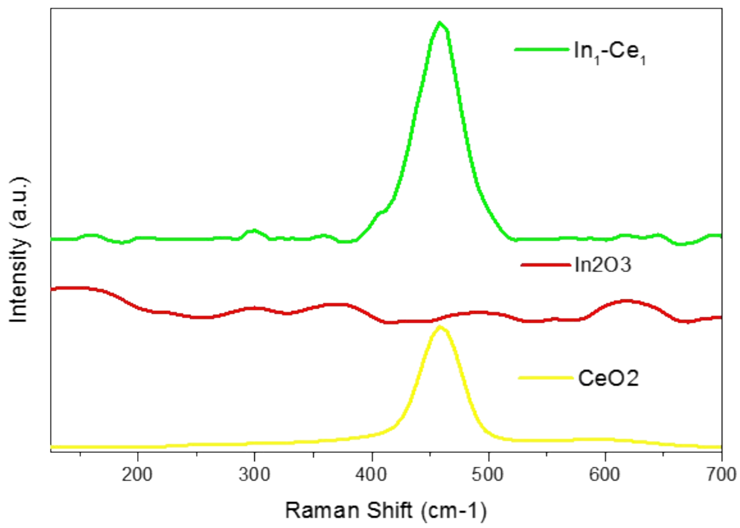

Figure S5. Raman spectra of In_1-Ce_1, In_2O_3 and CeO_2.

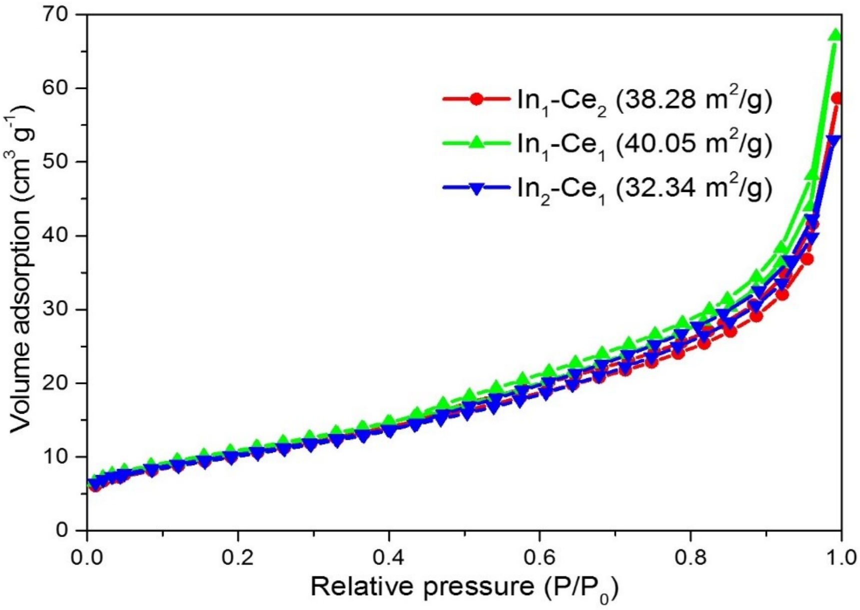

Figure S6. The nitrogen adsorption-desorption isotherms of the three catalysts, In_2-Ce_1, In_1-Ce_1, In_1-Ce_2 respectively.

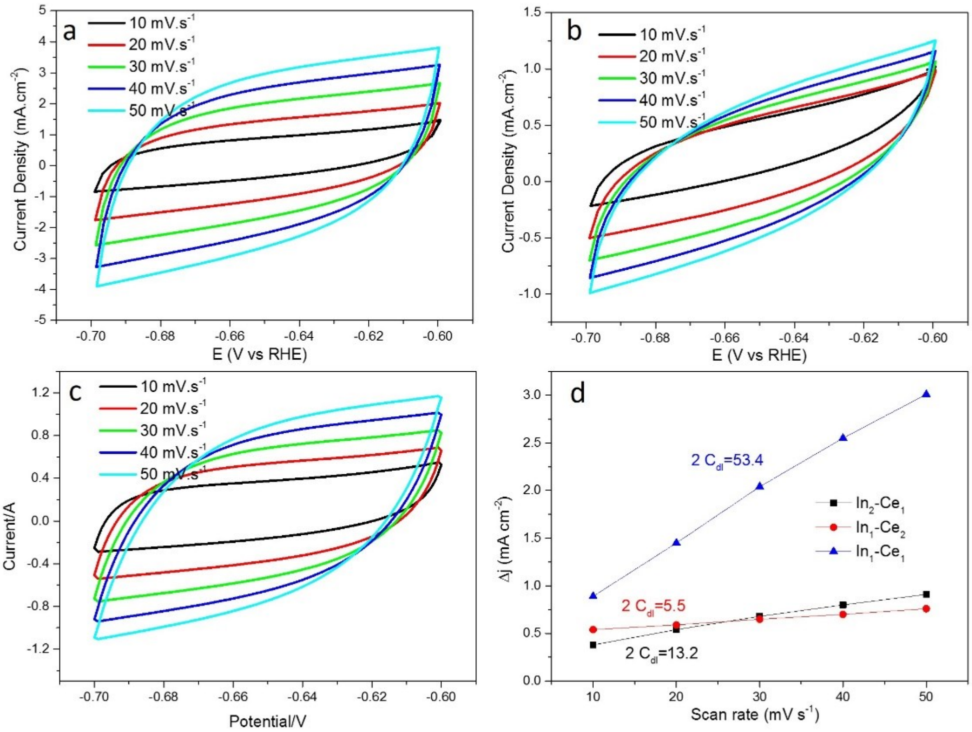

Figure S7. The cyclic voltammetry curves of (a) In_1-Ce_1 (b) In_1-Ce_2 (c) In_2-Ce_1 (d) the estimated C_{dl} values.

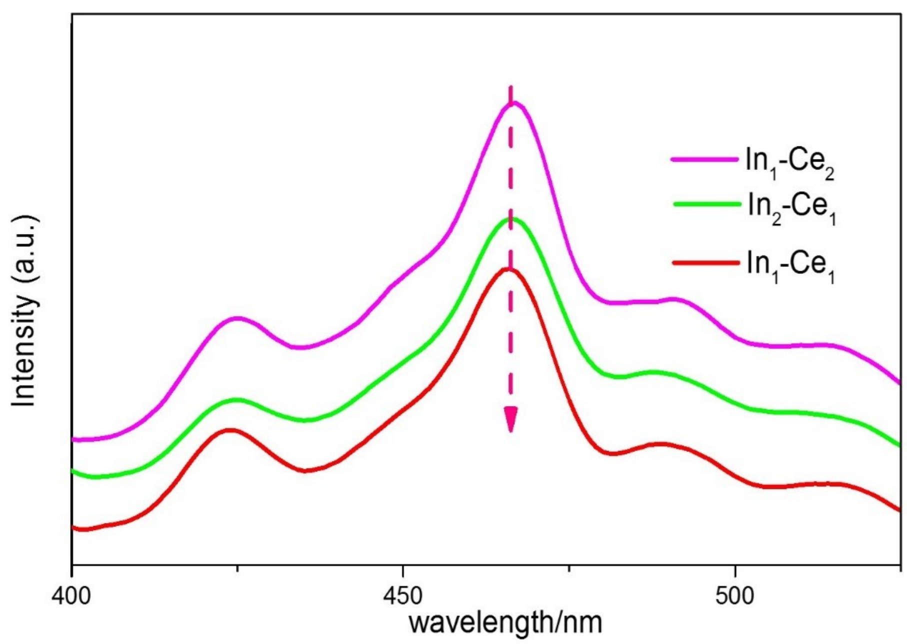

Figure S8. Photoluminescence spectra of the three catalysts.

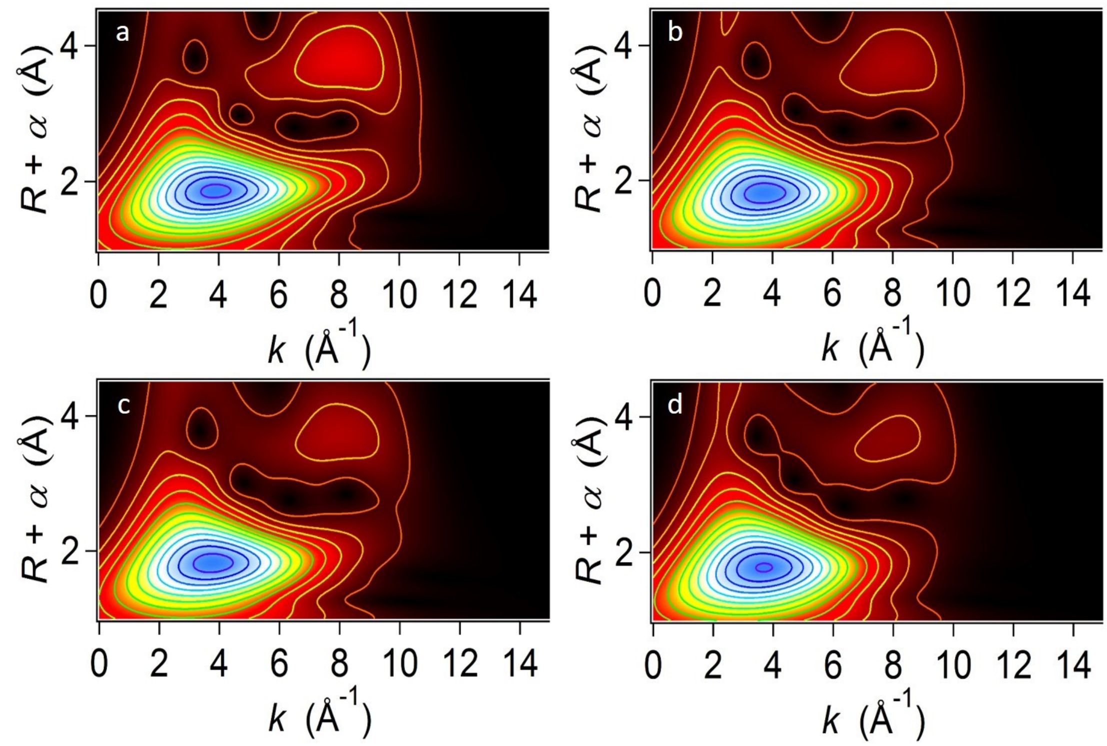

Figure S9. WT-EXAFS of Ce of the prepared catalysts CeO_2, In_2Ce_1, In_1Ce_2 and In_1Ce_1.

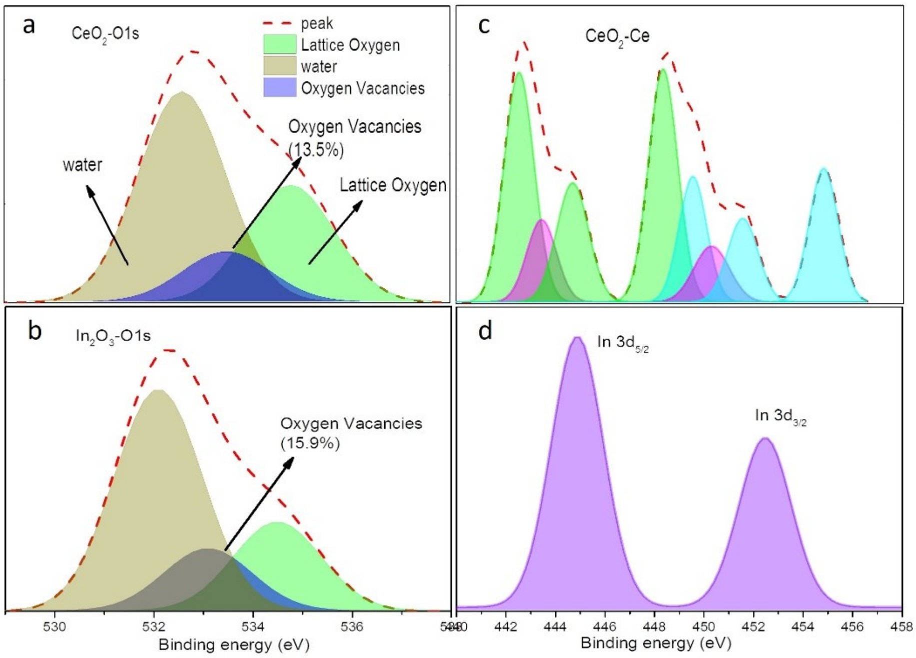

Figure S10. O1s XPS spectra of the (a) CeO_2 (b) In_2O_3. Ce spectra of (c) CeO_2. In 3d spectra of the (d) In_2O_3.

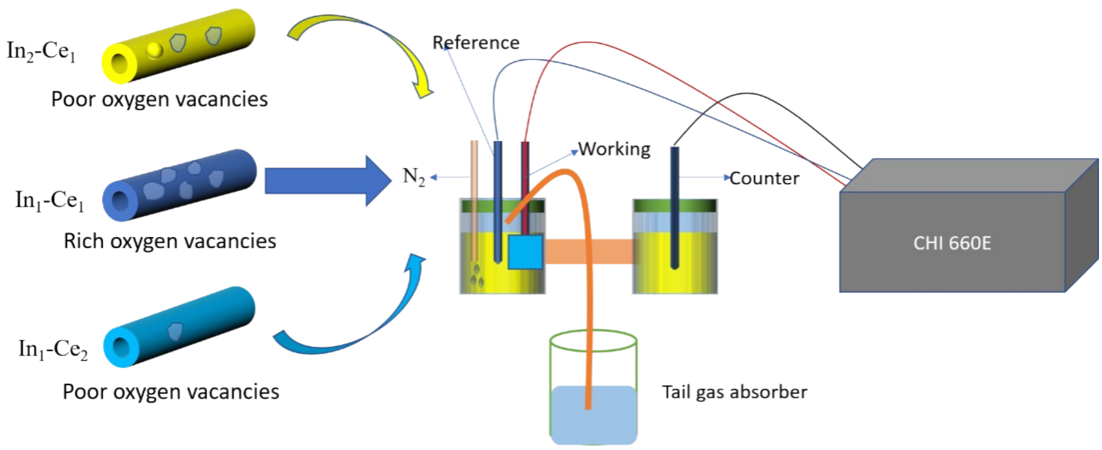

Figure S11. The schematic illustration for the electrocatalytic NRR process.

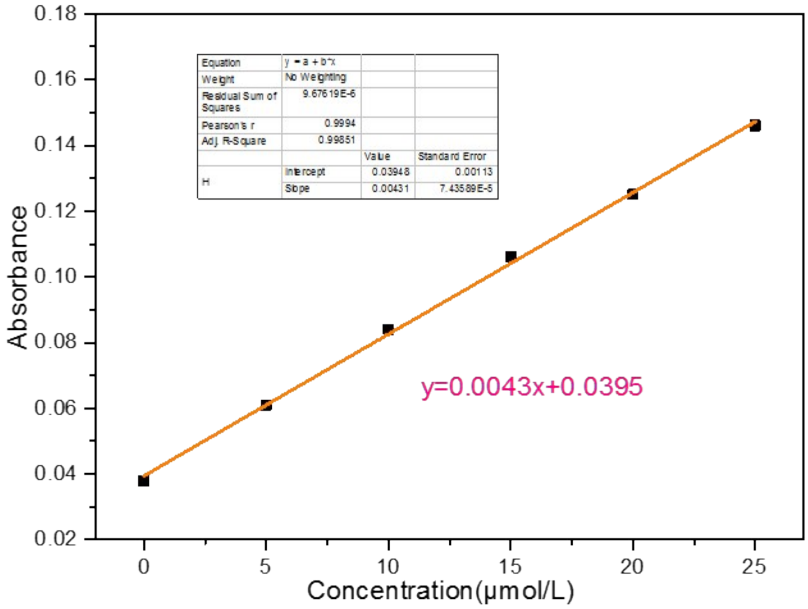

Figure S12. The standard curve of the NH_4Cl solution with various concentration.

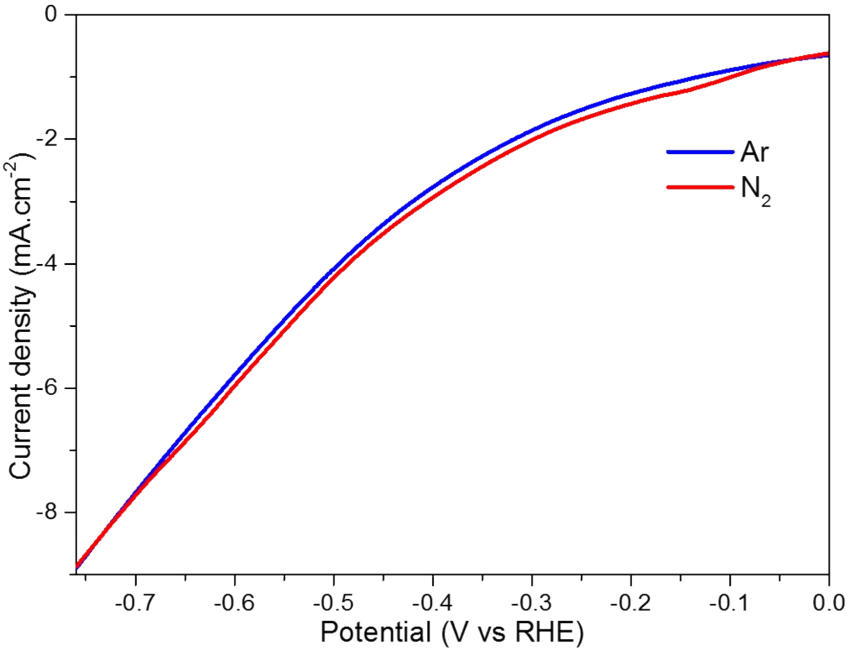

Figure S13. The linear sweep voltammetric curve of the catalyst In_1-Ce_1 in (pH=13) KOH aqueous solution under Ar and N_2 atmosphere.

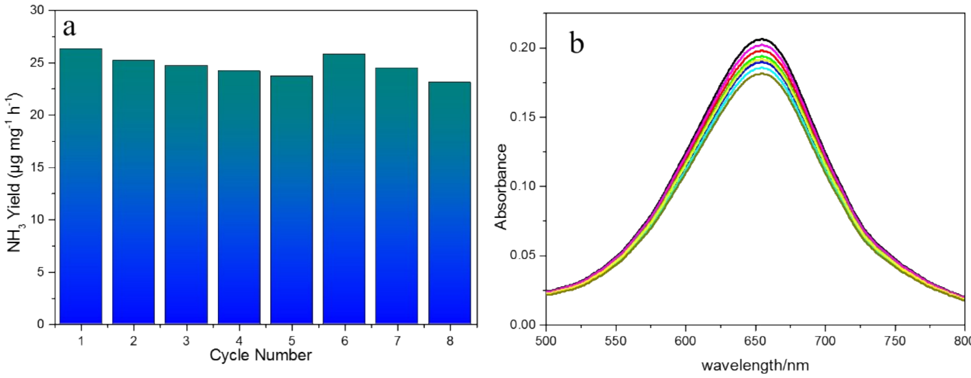

Figure S14. (a) The cycling test of the catalyst In_1-Ce_1 at -0.3 V versus RHE. (b) UV-vis curves of the catalyst In_1-Ce_1 corresponding to the cycling test.

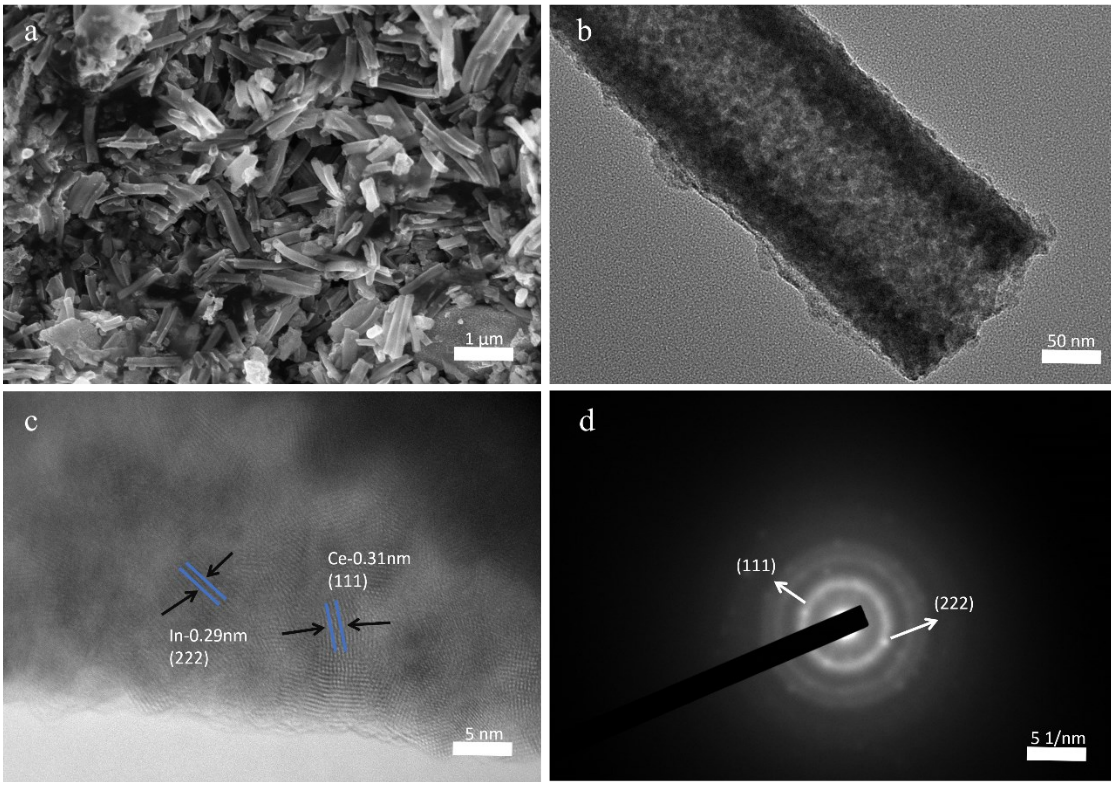

Figure S15. The images of the In_1-Ce_1 after the NRR (a) the SEM morphology. (b-c) the TEM images. (d) the HRTEM image.

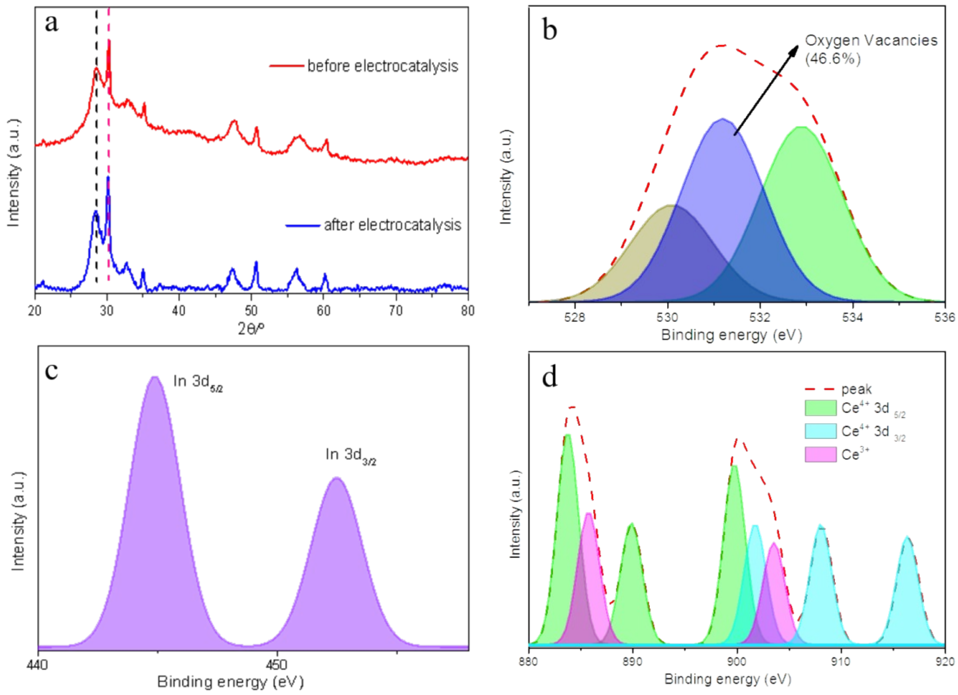

Figure S16. (a) the XRD patterns of the catalyst In_1-Ce_1 before and after the NRR. The XPS spectra of the In_1-Ce_1 after NRR: (b) O 1s (c) In 3d of the In_2O_3 (d) Ce^{3+} and 3d of the Ce^{4+}.

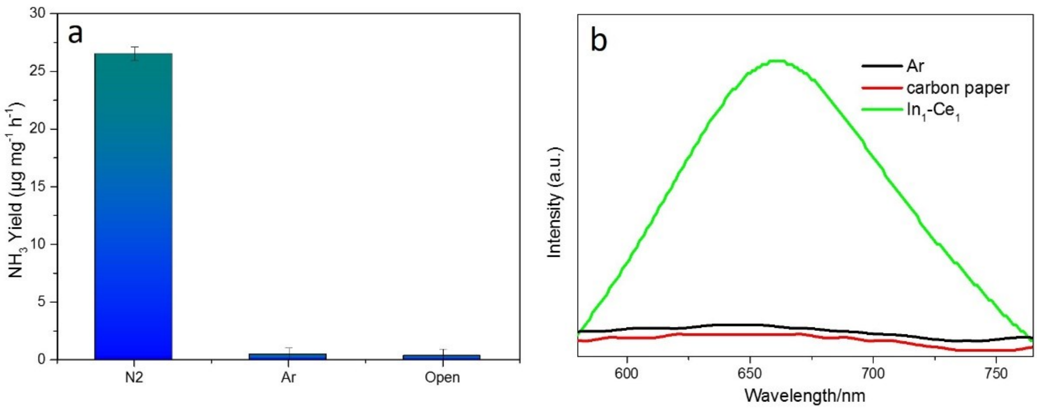

Figure S17. (a) the amount of NH_3 generated with different gas atmosphere after electrolysis at potential of -0.30 V under ambition condition. (b) the UV-vis curves of the catalyst In_1-Ce_1 at different conditions.

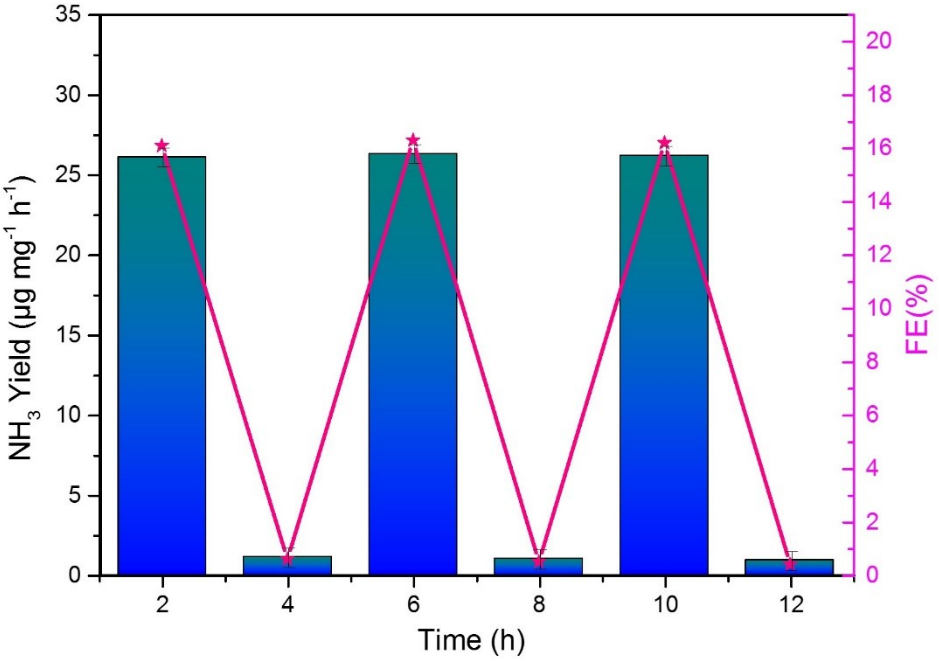

Figure S18. NH_3 yields and FEs of In_1-Ce_1 at the potential of -0.30 V with alternating 2h cycles between N_2-saturated electrolytes with a total of 12h.

Table S1. Comparison of the NH_3 yield rate and FE for In_1-Ce_1/CP with other NRR electrocatalysts at ambient condition

Catalyst	Electrode	NH_3 yield rate	FE(%)	Ref.
In_1-Ce_1	**0.1 M KOH**	**26.1μg h^{-1} $mg_{cat.-1}$**	**16.1**	**This work**
$Bi_4V_2O_{11}/CeO_2$	0.1M HCl	23.21μg h^{-1} $mg_{cat.-1}$	10.16	1
MoS_2/CC	0.1 M Na_2SO_4	4.94μg h^{-1} $mg_{cat.-1}$	1.17	2
a-Au/CeOx–RGO	0.1M HCl	8.3μg h^{-1} $mg_{cat.-1}$	10.10	3
Bi_5O_7Br	water	23.46μg h^{-1} $mg_{cat.-1}$	2.3	4
PCN	0.1M HCl	8.09 μg h^{-1} $mg_{cat.-1}$	11.59	5
Au NRs	0.1 M KOH	1.64 μg h^{-1} $cm_{cat.-1}$	3.88	6
Ru SAs/N-C	0.05M H_2SO_4	120.9μg h^{-1} $mg_{cat.-1}$	29.6	7
$Pd_{0.2}Cu_{0.8}$/rGO	0.1 M KOH	2.80μgh^{-1} $mg_{cat.-1}$	4.5	8
hollow Cr_2O_3 microspheres	0.1M Na_2SO_4	25.3μgh^{-1} $mg_{cat.-1}$	6.78	9
TiO_2-rGO	0.1M Na_2SO_4	15.13μgh^{-1} $mg_{cat.-1}$	3.3	10
Mn_3O_4 nanocube	0.1M Na_2SO_4	11.6μgh^{-1} $mg_{cat.-1}$	3.0	11
carbon nitride	0.1 M HCl	8.09μgh^{-1} $mg_{cat.-1}$	11.59	12
MoO_3	0.1 M HCl	29.43μgh^{-1} $mg_{cat.-1}$	1.9	13
defect-rich MoS_2	0.1M Na_2SO4	29.28μgh^{-1} $mg_{cat.-1}$	8.34	14
BG-1	0.05M H_2SO_4	9.8 μg h^{-1} cm^{-2}	10.8	15
NCM	0.1 M HCl	8 μg h^{-1} cm^{-2}	5.2	16
CNS	0.25 M Li2SO_4	97.18 μg h^{-1} cm^{-2}	11.56	17
Rh NNs	0.1 M KOH	23.88μgh^{-1} $mg_{cat.-1}$	0.217	18
AuHNCs	0.5 m $LiClO_4$	3.9 μg h^{-1} cm^{-2}	30.2	19

Reference

[1]. C. Lv, C. Yan, G. Chen, Y. Ding, J. Sun, Y. Zhou, G. Yu, *Angew Chem Int Ed Engl.*, 2018, **57**, 6073-6076.

[2]. L. Zhang, X. Ji, X. Ren, Y. Ma, X. Shi, Z. Tian, A. M. Asiri, L. Chen, B. Tang, X. Sun, *Adv Mater*, 2018, **30**, 1800191-1800196.

[3]. S. J. Li, D. Bao, M. M. Shi, B. R. Wulan, J. M. Yan, Q. Jiang, *Adv Mater*, 2017,

29, 1700001-1700006.

[4]. S. Wang, X. Hai, X. Ding, K. Chang, Y. Xiang, X. Meng, Z. Yang, H. Chen, J. Ye, *Adv Mater*, 2017, **29,** 1701774-1701780.

[5]. C. Lv, Y. Qian, C. Yan, Y. Ding, Y. Liu, G. Chen, G. Yu, *Angew Chem Int Ed Engl*, 2018, **57**, 10246-10250.

[6]. D. Bao, Q. Zhang, F. L. Meng, H. X. Zhong, M. M. Shi, Y. Zhang, J. M. Yan, Q. Jiang, X. B. Zhang, *Adv Mater*, 2017, **29,** 1604799-1604783.

[7]. Z. Geng, Y. Liu, X. Kong, P. Li, K. Li, Z. Liu, J. Du, M. Shu, R. Si, J. Zeng, *Adv Mater*, 2018, **4,** 1803498-1803453.

[8]. M.-M. Shi, D. Bao, S.-J. Li, B.-R. Wulan, J.-M. Yan, Q. Jiang, *Advanced Energy Materials*, 2018, **8**, 1800124-1800429.

[9]. Y. Zhang, W. Qiu, Y. Ma, Y. Luo, Z. Tian, G. Cui, F. Xie, L. Chen, T. Li, X. Sun, *ACS Catalysis*, 2018, **8**, 8540-8544.

[10]. X. Zhang, Q. Liu, X. Shi, A. M. Asiri, Y. Luo, X. Sun, T. Li, *Journal of Materials Chemistry A*, 2018, **6**, 17303-17306.

[11]. X. Wu, L. Xia, Y. Wang, W. Lu, Q. Liu, X. Shi, X. Sun, *Small*, 2018, e1803111.

[12]. C. Lv, Y. Qian, C. Yan, Y. Ding, Y. Liu, G. Chen, G. Yu, *Angew Chem Int Ed Engl*, 2018, **57**, 10246-10250.

[13]. J. Han, X. Ji, X. Ren, G. Cui, L. Li, F. Xie, H. Wang, B. Li, X. Sun, *Journal of Materials Chemistry A*, 2018, **6**, 12974-12977.

[14]. X. Li, T. Li, Y. Ma, Q. Wei, W. Qiu, H. Guo, X. Shi, *Advanced Energy Materials* 2018, **8**, 1801357.

[15]. Wang, H.; Wang, L.; Wang, Q.; Ye, S.; Sun, W.; Shao, Y.; Jiang, Z.; Qiao, Q.; Zhu, Y.; Song, P.; Li, D.; He, L.; Zhang, X.; Yuan, J.; Wu, T.; Ozin, G. A., *Angew Chem Int Ed Engl* **2018,** *57* (38), 12360-12364.

[16]. Nazemi, M.; Panikkanvalappil, S. R.; El-Sayed, M. A., *Nano Energy* **2018,** *49*, 316-323.

[17]. Liu, H.-M.; Han, S.-H.; Zhao, Y.; Zhu, Y.-Y.; Tian, X.-L.; Zeng, J.-H.; Jiang, J.-X.; Xia, B. Y.; Chen, Y., *Journal of Materials Chemistry A* **2018,** *6* (7), 3211-3217.

[18]. Guo, C.; Ran, J.; Vasileff, A.; Qiao, S.-Z., *Energy & Environmental Science* **2018,** *11* (1), 45-56.

[19]. Yang S, D. J., Rui P, Dale K. Hensley, Peter V. Bonnesen, Liangbo L,; Harry M. Meyer III, B. G. S., 1,2 Adam J. Rondinone1, *Science Advance* **2018,** *4*, e1700336.